International Journal of Engineering, Mathematical and Physical Sciences
ISSN: 2517-9934
Vol:7, No:11, 2013

Bernstein-Galerkin Approach for Perturbed Constant-Coefficient Differential Equations, One-Dimensional Analysis

Diego Garijo

Abstract—A numerical approach for solving constant-coefficient differential equations whose solutions exhibit boundary layer structure is built by inserting Bernstein Partition of Unity into Galerkin variational weak form. Due to the reproduction capability of Bernstein basis, such implementation shows excellent accuracy at boundaries and is able to capture sharp gradients of the field variable by p-refinement using regular distributions of equi-spaced evaluation points. The approximation is subjected to convergence experimentation and a procedure to assemble the discrete equations without a background integration mesh is proposed.

Keywords—Bernstein polynomials, Galerkin, differential equation, boundary layer.

I. Introduction

IN recent years, Bernstein polynomials [1] have been tested with success as trial functions for boundary value problems. The implementation of Bernstein expansion into a Galerkin scheme provides a meshfree-type approximation [2] with smooth globally-supported shape functions that present interesting properties related to consistency and reproduction capability [3]. Bernstein polynomials constitute a Partition of Unity (PU) by themselves and their derivatives [4] satisfy the Partition of Nullity (PN) property [5]. Furthermore, they form a complete basis of the polynomial space allowing the reproduction of any bounded continuous function by uniform convergence as the order of the basis is increased [1].

Computational tests have proved the feasibility of the application of Bernstein polynomials to solve differential equations with highly-accurate results. Bhatti and Bracken [6] posed the combination of Bernstein basis functions and expansion coefficients to approximate the solutions to differential equations. Further work related to the study of elliptic boundary value problems was published by Mirkov and Rasuo [7]. Interface value problems were reviewed by J. Liu *et al.* [8], while Bernstein-Galerkin and Bernstein-Petrov-Galerkin formulations were applied to high even-order differential equations by Doha *et al.* [4]. Numerical behavior for free vibration analysis was tested by Valencia *et al.* [5], and comparison of computational performances between Bernstein and Moving Least Squares (MLS) [9] approximations in elasto-statics benchmarks was presented by Garijo *et al.* [10]. Other global spectral-type expansions [11][12] like Lagrange basis have also been introduced as shape functions of modified Element-Free Galerkin Methods (EFGM) [13][14], yielding excellent results in terms of numerical error as reported by Ohkami *et al.* [15] and Suetake [16].

D. Garijo is with the Department of Structural Analysis, Safran Engineering Services (Safran Group). Calle Arnaldo de Vilanova, 5, 28906. Getafe, Madrid (Spain). (e-mail: diego.garijo@safran-engineering.com).

Bernstein expansion leads to analytical global shape functions extended to the whole domain of definition. Convergence is achieved by means of p-refinement instead of the h-refinement —or mesh refinement—, which is the classical strategy of mesh-based approximations like Finite Element Method (FEM) [17] to reproduce local high-order solutions, e.g. stress concentration factors in solid mechanics or confined boundary layers in convection-diffusion problems. In a Bernstein-Galerkin approach, the order of the global approximation is directly determined by the order selected for Bernstein basis and the expansion can be performed with patterns of equi-spaced evaluation points, which simplifies the programing. Moreover, due to the non-interpolating nature of Bernstein polynomials, the expansion avoids the Runge phenomenon [18] and detrimental saturation that affects to the schemes that employ high-order Lagrange interpolation with equi-spaced nodes.

In this context, this work discusses the computational performance of Bernstein-Galerkin approach when dealing with boundary layer solutions [19] to constant-coefficient differential equations with small perturbing parameters. The weak form of these equations is developed and discretized. Numerical experiments test the accuracy and the convergence of the results.

II. Bernstein polynomials

For a given function $f(x)$ defined in the interval $x \in$ [0,1], its Bernstein polynomial of order p is defined as [1]:

$$B_p^f(x) = \sum_{i=0}^{p} f\left(\frac{i}{p}\right)\binom{p}{i} x^i (1-x)^{p-i} \tag{1}$$

The set of Bernstein basis functions

$$B_i^p(x) = \binom{p}{i} x^i (1-x)^{p-i} \tag{2}$$

constitutes a Partition of Unity (PU) of order 1 for patterns of equi-spaced evaluation points [5]:

$$\sum_{i=0}^{p} B_i^p(x) x_i^m = 1 \quad , \quad m = 0, 1 \quad , \quad x_i = i/p \tag{3}$$

and is able to reproduce any continuous and bounded function $f(x)$ in the interval [0,1] by uniform convergence [18]:

$$\lim_{p\to\infty} B_p^f(x) = f(x) \tag{4}$$

Bernstein basis (see Fig. 1) can be used to generate a set of shape functions usable in a Galerkin implementation. Let $u(x)$ be a function defined in a one-dimensional domain Ω, which is intended to be approximated by a numerical function $u^h(x)$ resulting from the linear combination:

$$u^h(x) = \sum_{i=1}^{n} B_i(x)\, a_i \tag{5}$$

where n is the number of evaluation points in the domain, B_i is the shape function associated to point i and a_i is the i-th evaluation point parameter, which is not the actual field variable value at evaluation point i, since Bernstein expansion does not possess the Kronecker delta property, $a_i \neq u^h(x_i)$, as it is not an interpolation scheme. Kronecker delta property is satisfied only at the extremes of the interval, $B_1(x_j) = \delta_{1j}$, $B_n(x_j) = \delta_{nj}$, being $x_1 = 0$ and $x_n = 1$.

The shape function B_i is therefore written in the form:

$$B_i(x) = B_{i-1}^{n-1}(x) = \binom{n-1}{i-1} x^{i-1}(1-x)^{n-i} \tag{6}$$

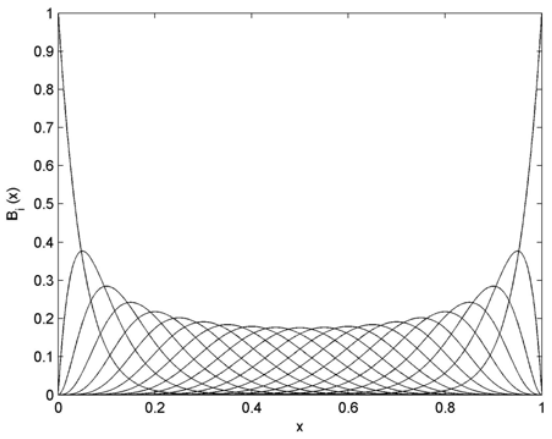

Fig. 1. Bernstein basis functions, 21 evaluation points

As stated in [10], the computational cost of Bernstein implementation is closely related to the evaluation of binomial terms of high orders. Following Mirkov and Rasuo [7] and Spivey [20], binomial terms may be computed more efficiently by applying the Binomial Multiplicative formula:

$$\binom{m}{l} = \prod_{h=1}^{l} \frac{m-(l-h)}{h} \tag{7}$$

then:

$$B_i(x) = \left(\prod_{h=1}^{i-1} \frac{n-i+h}{h}\right) x^{i-1}(1-x)^{n-i} \tag{8}$$

The derivatives of Bernstein shape functions (Fig. 2) can be expressed as [10]:

$$\frac{dB_i}{dx} = \frac{i-1-(n-1)\,x}{x\,(1-x)} B_i \quad , \quad x \neq 0,1 \tag{9}$$

$$\frac{dB_i}{dx} = \begin{cases} \mp(n-1) & \text{if } i-1 = 0,1; \\ 0 & \text{if } i-1 \neq 0,1. \end{cases} \quad , \quad x = 0 \tag{10}$$

$$\frac{dB_i}{dx} = \begin{cases} \mp(n-1) & \text{if } i-1 = n-2, n-1; \\ 0 & \text{if } i-1 \neq n-2, n-1. \end{cases} \quad , \quad x = 1 \tag{11}$$

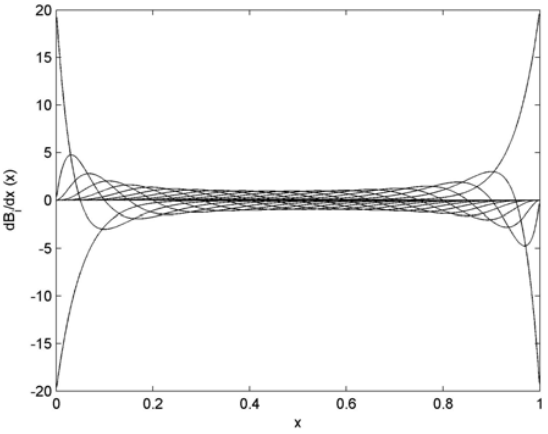

Fig. 2. Derivatives of Bernstein basis functions, 21 evaluation points

By defining the inner product $P(f,g)$

$$P(f,g) = \langle f,g \rangle = \int_0^1 fg\,dx \tag{12}$$

and the integral $I_t(\alpha,\beta)$:

$$\begin{aligned} I_t(\alpha,\beta) &= \int t^{\alpha}(1-t)^{\beta}\,dt = \\ &= \sum_{k=0}^{\beta} \binom{\beta}{k} 1^{\beta-k}(-1)^k \frac{t^{\alpha+k+1}}{\alpha+k+1} \end{aligned} \tag{13}$$

it is verified that Bernstein basis is not orthogonal:

$$\begin{aligned} P(B_i,B_j) &= \int_0^1 B_i B_j\,dx = \\ &= \gamma_{i,j}^n\, I_x(i+j-2, 2n-i-j)\big|_0^1 \neq \delta_{ij}\, \|P(B_i,B_j)\| \end{aligned} \tag{14}$$

where $\gamma_{i,j}^n = \binom{n-1}{i-1}\binom{n-1}{j-1}$. Interesting expressions can however be derived by extending the inner product to the derivatives (9)-(11):

$$\begin{aligned} P\left(\frac{dB_i}{dx}, B_j\right) &= \int_0^1 \frac{dB_i}{dx} B_j\,dx = \\ &= \gamma_{i,j}^n \Big[(i-1)\, I_x(i+j-3, 2n-i-j-1)\big|_0^1 - \\ &\quad - (n-1)\, I_x(i+j-2, 2n-i-j-1)\big|_0^1 \Big] \end{aligned} \tag{15}$$

$$P\left(\frac{dB_i}{dx},\frac{dB_j}{dx}\right)=\int_0^1\frac{dB_i}{dx}\frac{dB_i}{dx}dx=$$
$$=\gamma_{i,j}^n\left[(i-1)(j-1)I_x(i+j-4,2n-i-j-2)|_0^1-\right.$$
$$-(i+j-2)(n-1)I_x(i+j-3,2n-i-j-2)|_0^1+$$
$$\left.+(n-1)^2I_x(i+j-2,2n-i-j-2)\Big|_0^1\right] \tag{16}$$

Previous expressions can be used to compute the terms of the matrices of Galerkin weak form without need of a background integration mesh.

III. Galerkin weak form for one-dimensional perturbation problems

The boundary value problem considered for analysis is:

$$A(\varepsilon)\frac{d^2u}{dx^2}+B(\varepsilon)\frac{du}{dx}+C(\varepsilon)u=g(x)\quad,\quad\varepsilon<<1 \tag{17}$$

$$u(0)=\bar{u}_0\quad,\quad u(1)=\bar{u}_1 \tag{18}$$

The governing differential equation (17) is the general form of a non-homogeneous constant-coefficient second-order differential equation with small perturbing parameter ε. Typically, when the highest derivative is multiplied by the perturbing parameter ($A(\varepsilon)=\varepsilon$), the solution to (17) presents narrow regions of very sharp gradients to adapt to the imposed boundary conditions (18), this is, exhibits boundary layer structure [19]. The problem (17)-(18) is a classical mathematical model of one-dimensional convection-diffusion phenomena, which have been widely studied with numerical approximations, including finite difference, finite element and meshless techniques, see Morton and Mayers [21], Miller *et al.* [22], Budd *et al.* [23], Knobloch [24] and recent works by Roos *et al.* [25] and Reddy *et al.* [26].

The weak form of equation (17) is posed by introducing a virtual field δU and enforcing the integral:

$$\int_0^1\delta U\left\{A(\varepsilon)\frac{d^2u}{dx^2}+B(\varepsilon)\frac{du}{dx}+C(\varepsilon)u-g(x)\right\}dx=0 \tag{19}$$

The term of (19) multiplied by the perturbing coefficient $A(\varepsilon)$ can be developed as:

$$\int_0^1\delta U\frac{d^2u}{dx^2}dx=\left[\delta U\frac{du}{dx}\Big|_0^1-\int_0^1\frac{d\delta U}{dx}\frac{du}{dx}dx\right] \tag{20}$$

Essential boundary conditions (18) are enforced by means of Lagrange Multipliers, which is a classical strategy for approximations that do not verify the Kronecker delta property [2]. The additional set of unknowns to be introduced in the weak form (19) are:

$$\boldsymbol{\lambda}^T=(\lambda_0\quad\lambda_1)\quad,\quad\boldsymbol{\delta\lambda}^T=(\delta\lambda_0\quad\delta\lambda_1) \tag{21}$$

therefore

$$\delta U\frac{du}{dx}\Big|_0^1=\delta U(1)\lambda_1+\delta\lambda_1(u-\bar{u}_1)|_{x=1}-$$
$$-\delta U(0)\lambda_0-\delta\lambda_0(u-\bar{u}_0)|_{x=0} \tag{22}$$

and the weak form (19) becomes:

$$A(\varepsilon)\{\delta U(1)\lambda_1+\delta\lambda_1u(1)-\delta\lambda_1\bar{u}_1-$$
$$-\delta U(0)\lambda_0-\delta\lambda_0u(0)+\delta\lambda_0\bar{u}_0\}-$$
$$-A(\varepsilon)\int_0^1\frac{d\delta U}{dx}\frac{du}{dx}dx+B(\varepsilon)\int_0^1\delta U\frac{du}{dx}dx+$$
$$+C(\varepsilon)\int_0^1\delta Uudx-\int_0^1\delta Ug(x)dx=0 \tag{23}$$

The Galerkin scheme employs the Bernstein basis to approximate both the trial and the test fields using (5):

$$u=\sum_{i=1}^nB_i(x)a_i\quad,\quad\delta U=\sum_{j=1}^nB_j(x)\delta a_j \tag{24}$$

Inserting now the expressions (24) into (23):

$$A(\varepsilon)\left\{\sum_{j=1}^nB_j(x=1)\delta a_j\lambda_1+\delta\lambda_1\sum_{i=1}^nB_i(x=1)a_i-\right.$$
$$-\delta\lambda_1\bar{u}_1-\sum_{j=1}^nB_j(x=0)\delta a_j\lambda_0-$$
$$\left.-\delta\lambda_0\sum_{i=1}^nB_i(x=0)a_i+\delta\lambda_0\bar{u}_0\right\}-$$
$$-A(\varepsilon)\int_0^1\left[\left(\sum_{j=1}^n\frac{dB_j}{dx}\delta a_j\right)\left(\sum_{i=1}^n\frac{dB_i}{dx}a_i\right)\right]dx+$$
$$+B(\varepsilon)\int_0^1\left[\left(\sum_{j=1}^nB_j(x)\delta a_j\right)\left(\sum_{i=1}^n\frac{dB_i}{dx}a_i\right)\right]dx+$$
$$+C(\varepsilon)\int_0^1\left[\left(\sum_{j=1}^nB_j(x)\delta a_j\right)\left(\sum_{i=1}^nB_i(x)a_i\right)\right]dx-$$
$$-\int_0^1\left(\sum_{j=1}^nB_j(x)\delta a_j\right)g(x)dx=0 \tag{25}$$

Defining the arrays:

$$\mathbf{B}^T=(B_1\quad B_2\quad\dots\quad B_n) \tag{26}$$

$$\mathbf{a}^T=(a_1\quad a_2\quad\dots\quad a_n) \tag{27}$$

$$\boldsymbol{\delta}\mathbf{a}^T=(\delta a_1\quad\delta a_2\quad\dots\quad\delta a_n) \tag{28}$$

equation (25) can be expressed in compact form:

$$\boldsymbol{\delta}\mathbf{a}^TA(\varepsilon)\mathbf{B}_j(x=1)\lambda_1+\delta\lambda_1A(\varepsilon)\mathbf{B}_i^T(x=1)\mathbf{a}-$$
$$-\boldsymbol{\delta}\mathbf{a}^TA(\varepsilon)\mathbf{B}_j(x=0)\lambda_0-\delta\lambda_0A(\varepsilon)\mathbf{B}_i^T(x=0)\mathbf{a}-$$
$$-\delta\lambda_1A(\varepsilon)\bar{u}_1+\delta\lambda_0A(\varepsilon)\bar{u}_0-$$
$$-\boldsymbol{\delta}\mathbf{a}^TA(\varepsilon)\int_0^1\left[\frac{d\mathbf{B}_j}{dx}\frac{d\mathbf{B}_i^T}{dx}\right]dx\mathbf{a}+$$
$$+\boldsymbol{\delta}\mathbf{a}^TB(\varepsilon)\int_0^1\left[\mathbf{B}_j\frac{d\mathbf{B}_i^T}{dx}\right]dx\mathbf{a}+$$
$$+\boldsymbol{\delta}\mathbf{a}^TC(\varepsilon)\int_0^1\left[\mathbf{B}_j\mathbf{B}_i^T\right]dx\mathbf{a}-\boldsymbol{\delta}\mathbf{a}^T\int_0^1\mathbf{B}_jg(x)dx=0 \tag{29}$$

Solving (29) for all $\boldsymbol{\delta}\mathbf{a}$ and $\boldsymbol{\delta}\boldsymbol{\lambda}$ fields:

$$\begin{gathered} -\mathbf{K}^{\varepsilon}\mathbf{a}+\mathbf{D}^{\varepsilon}\mathbf{a}+\mathbf{M}^{\varepsilon}\mathbf{a}-\mathbf{g}+ \\ +A(\varepsilon)\mathbf{B}_j(x=1)\lambda_1+A(\varepsilon)\mathbf{B}_j(x=0)\lambda_0=0 \end{gathered} \tag{30}$$

$$\begin{aligned} A(\varepsilon)\mathbf{B}(x=0)\mathbf{a}-A(\varepsilon)\bar{u}_0=0 \\ A(\varepsilon)\mathbf{B}(x=1)\mathbf{a}-A(\varepsilon)\bar{u}_1=0 \end{aligned} \tag{31}$$

Finally, expressions (30) and (31) can be compacted as:

$$\begin{bmatrix} \mathbf{K}^{\varepsilon}-\mathbf{D}^{\varepsilon}-\mathbf{M}^{\varepsilon} & \mathbf{G}^{\varepsilon} \\ \mathbf{G}^{\varepsilon T} & \mathbf{0} \end{bmatrix} \begin{Bmatrix} \mathbf{a} \\ \boldsymbol{\lambda} \end{Bmatrix} = \begin{Bmatrix} -\mathbf{g} \\ -\bar{\mathbf{u}}^{\varepsilon} \end{Bmatrix} \tag{32}$$

where the terms in the matrices are:

$$\begin{aligned} \mathbf{K}^{\varepsilon}_{ij} &= A(\varepsilon)\int_0^1 \frac{dB_i}{dx}\frac{dB_j}{dx}dx \\ \mathbf{D}^{\varepsilon}_{ij} &= B(\varepsilon)\int_0^1 \frac{dB_i}{dx}B_j dx \\ \mathbf{M}^{\varepsilon}_{ij} &= C(\varepsilon)\int_0^1 B_i B_j dx \\ \mathbf{G}^{\varepsilon}_{ik} &= -A(\varepsilon)B_i(x=x_k) \\ \mathbf{g}_i &= \int_0^1 \mathbf{B}_i g(x)\,dx \\ \bar{\mathbf{u}}^{\varepsilon}_k &= A(\varepsilon)\bar{u}_k \end{aligned} \tag{33}$$

The integrals of $\mathbf{M}_{ij}$, $\mathbf{D}_{ij}$ and $\mathbf{K}_{ij}$ in (31) can be computed exactly using expressions (14), (15) and (16), respectively. A background integration mesh for numerical integration is therefore not required, then the order of the quadrature, for instance the number of Gauss points, is not a parameter of the Bernstein-Galerkin approach. For the particular case in which $g(x)$ is a polynomial function, an exact expression for the term $\mathbf{g}_i$ can also be derived using (13):

$$\begin{aligned} \mathbf{g}_i &= \int_0^1 \mathbf{B}_i\left(\sum_{h=0}^{H} g_h x^h\right)dx = \sum_{h=0}^{H} g_h \int_0^1 \mathbf{B}_i x^h dx = \\ &= \sum_{h=0}^{H} g_h \binom{n-1}{i-1}\int_0^1 x^{i-1+h}(1-x)^{n-i}dx = \\ &= \sum_{h=0}^{H} g_h \binom{n-1}{i-1} I_x(i-1+h, n-i)\Big|_0^1 \end{aligned} \tag{34}$$

IV. Numerical experiments

In this section, the exposed Bernstein-Galerkin approach is tested in reference cases of bibliography. The experiments deal with the response of the approximation scheme in terms of numerical error and convergence when the perturbing parameter ε is modified. The accuracy of the approach is evaluated with the global norm of error E, defined as:

$$E = log\left\{\sqrt{\frac{1}{2}\int_0^1 \left(u^{exact}(x)-u^{num}(x)\right)^2}\right\} \tag{35}$$

where u^{exact} and u^{num} are the exact and the numerical solutions, respectively.

A. Exactly Soluble Boundary Layer Problem

The first analysis is performed for the perturbed differential equation:

$$\varepsilon\frac{d^2u}{dx^2}+(1+\varepsilon)\frac{du}{dx}+u=0 \quad , \quad \varepsilon << 1 \tag{36}$$

with boundary conditions $u(0)=0, u(1)=1$. The exact solution can be found in Bender and Orszag [19] or Johnson [27]:

$$u^{exact}(x) = \frac{e^{-x}-e^{-x/\varepsilon}}{e^{-1}-e^{-1/\varepsilon}} \tag{37}$$

The solution presents a boundary layer in the left extreme $x=0$ of the interval. The thickness of the region where boundary layer is confined, the so-called *inner region*, becomes proportional to ε as $\varepsilon \to 0$. Note that the Taylor serie of $e^{-x/\varepsilon}$ up to order m as $x \to 0$ is:

$$e^{-x/\varepsilon} = 1+\sum_{i=1}^{m}(-1)^i\frac{x^i}{\varepsilon^i i!}+O\left(\frac{x^{m+1}}{\varepsilon^{m+1}}\right) \tag{38}$$

and therefore the numerical approach should be able to reproduce in the *inner region* a polynomial function whose coefficients are $\sim(1/\varepsilon^m)$.

The exact and Bernstein-Galerkin solutions are plotted in Fig. 3 and Fig. 4 for two different values of ε:

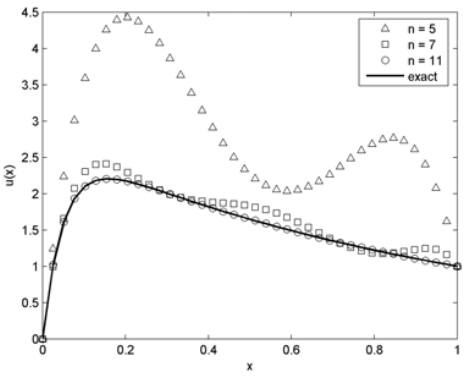

Fig. 3. Exact and numerical solutions, ε = 0.05, analysis case A

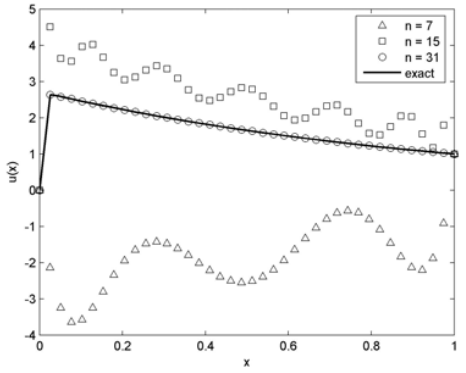

Fig. 4. Exact and numerical solutions, ε = 0.005, analysis case A

The norm of error (35) for the first reference case is presented in Fig. 5 as a function of the number of evaluation points n (note that the order of the Bernstein expansion is therefore $n-1$):

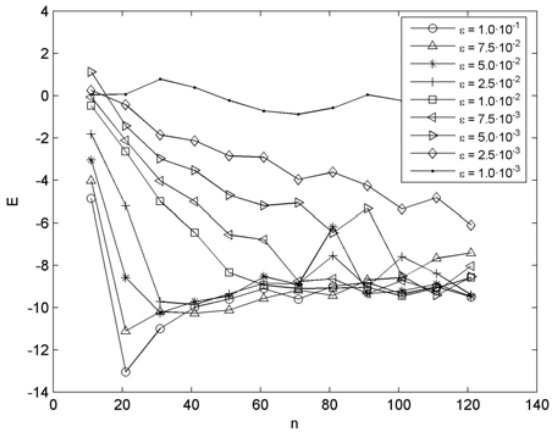

Fig. 5. Norm of error E, analysis case A

The analysis of Fig. 5 reveals interesting features of the numerical behavior of the Bernstein-Galerkin approach. First, for the range of ε from 10^{-1} to $2.5{\cdot}10^{-2}$, the norm E reaches a minimum for moderately low number of equi-spaced evaluation points n, and afterwards the approximation becomes less accurate and E tends asymptotically to a value of $E \sim -9$, which is still an excellent result. This phenomenon suggests that when the boundary layer gradient is relatively smooth, the numerical approximation provides very accurate results that are not improved by further increase of the order of the polynomial basis. Similar behavior was found in Garijo *et al.* [10], where the lack of convergence with p-refinement was attributed to truncation errors and to the evaluation of powers of high order when building Bernstein shape functions. Second, for lower values of ε, this is, for thinner boundary layer regions, the approximation is convergent and accurate results can be reached, although the rates of convergence become slower as ε decreases. Note that the numerical approach is compared in this case versus the exact solution of (36).

B. Boundary Layers at Both Ends of the Interval

The second reference case is a classical example of exponentially decaying solutions for $x \to 0$ and $x \to 1$, resulting in boundary layers at both ends of the interval in order to satisfy the boundary conditions. The non-homogeneous governing differential equation is:

$$\varepsilon^2 \frac{d^2u}{dx^2} - u = -1 \quad , \quad \varepsilon << 1 \tag{39}$$

with boundary conditions $u(0) = 0, u(1) = 0$. The analytical first-order solution is provided by Hinch [28]:

$$u^{exact}(x) \sim 1 - e^{-x/\varepsilon} - e^{(x-1)/\varepsilon} \tag{40}$$

Similarly to previous case, the Bernstein-Galerkin approach is tested by sweeping parameters ε and n. Figures that follow illustrate the numerical behaviour of the numerical approach:

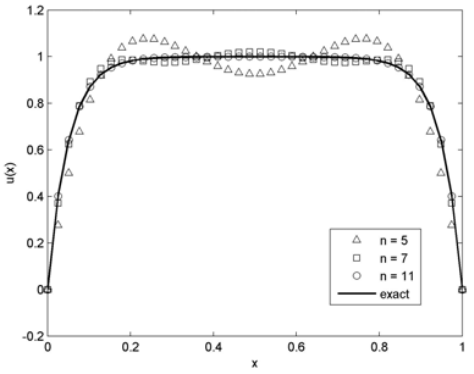

Fig. 6. Exact and numerical solutions, ε = 0.05, analysis case B

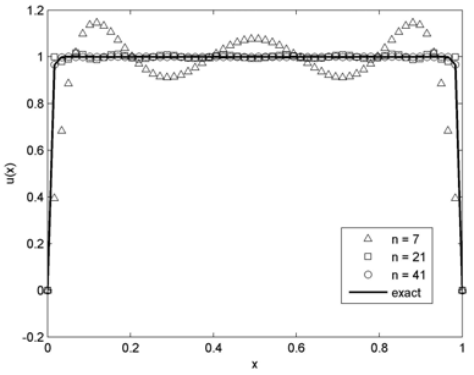

Fig. 7. Exact and numerical solutions, ε = 0.005, analysis case B

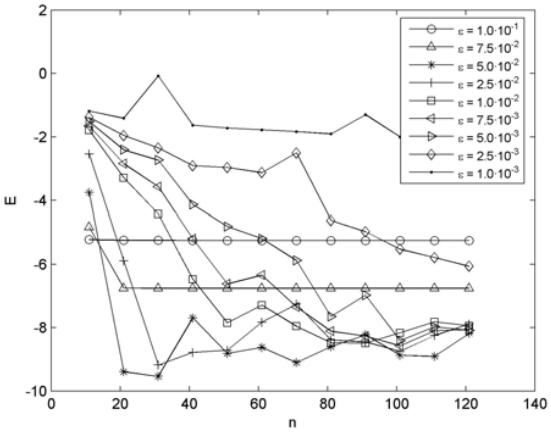

Fig. 8. Norm of error E, analysis case B

Expression (40) is a first-order solution to (39), therefore for perturbing parameter ε not too small, numerical solutions

may be noticeably closer to the actual full solution to (39) than (40). In Fig. 8, this feature is confirmed by the constant error curves obtained for $\varepsilon = 10^{-1}$ and ε =7.5·10^{-2}. For lower values of ε, the refinement of solution (40) allows the numerical behavior of case A to be recovered. The rate of converge of Bernstein-Galerkin approach with n decreases progresively with ε, although many of the curves tend to error $E \sim -9$.

C. Second-Order Approximation for Two-Point Boundary Value Problem with Smooth Forcing Term $g(x)$

The third analysis focuses on the equation:

$$\varepsilon \frac{d^2u}{dx^2} - u = g(x) \quad , \quad \varepsilon << 1 \tag{41}$$

with boundary conditions $u(0) = 0, u(1) = 0$ and function $g(x)$ sufficiently smooth on $[0,1]$. Verhulst [29] gives a second-order formal uniform expansion for (41) by adding the *outer* and *inner* (boundary layer) regions terms:

$$u^{exact}(x) = -g(x) + g(0)\, e^{\frac{-x}{\sqrt{\varepsilon}}} + g(1)\, e^{\frac{-(1-x)}{\sqrt{\varepsilon}}} + \\ + \sqrt{\varepsilon}\frac{d^2g}{dx^2}(0)\, e^{\frac{-x}{\sqrt{\varepsilon}}} + \sqrt{\varepsilon}\frac{d^2g}{dx^2}(1)\, e^{\frac{-(1-x)}{\sqrt{\varepsilon}}} + O(\varepsilon) \tag{42}$$

For numerical experimentation, two functions $g(x)$ are selected, $g(x) = x^3$ (case C1) and $g(x) = cos(x)$ (case C2):

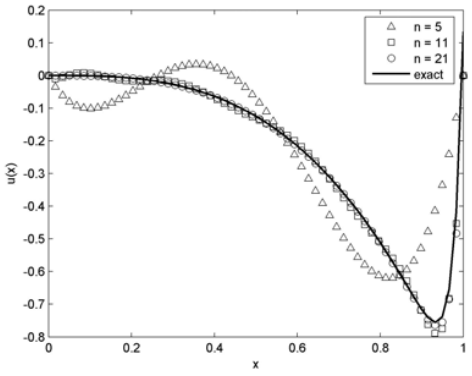

Fig. 9. Exact and numerical solutions, ε = 0.0005, analysis case C1

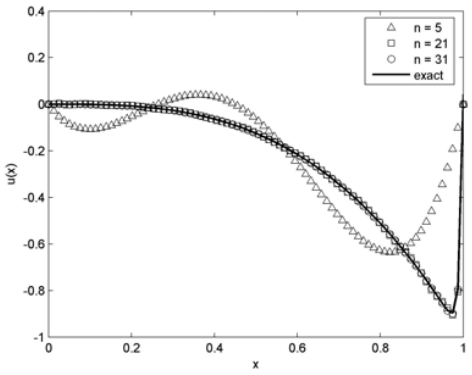

Fig. 10. Exact and numerical solutions, ε = 0.00005, analysis case C1

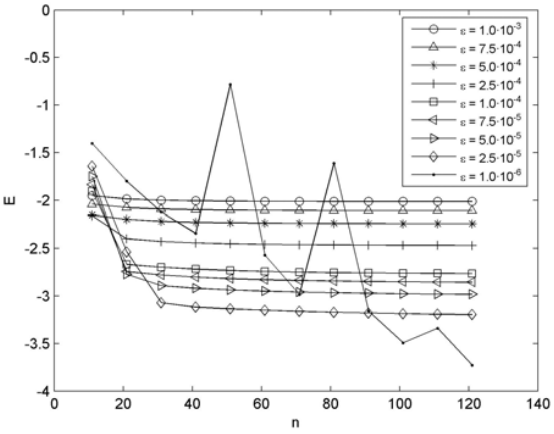

Fig. 11. Norm of error E, ε 10^{-3} to 10^{-6}, analysis case C1

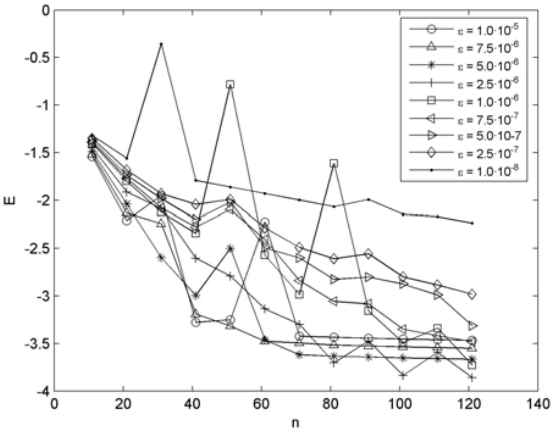

Fig. 12. Norm of error E, ε 10^{-5} to 10^{-8}, analysis case C1

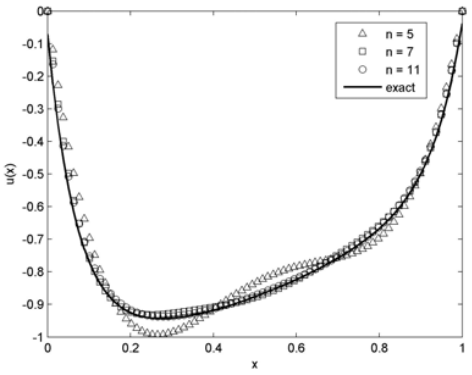

Fig. 13. Exact and numerical solutions, ε = 0.005, analysis case C2

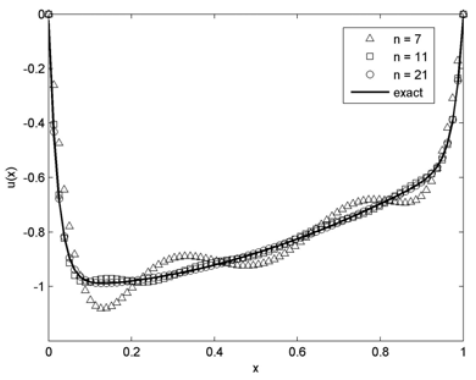

Fig. 14. Exact and numerical solutions, ε = 0.0005, analysis case C2

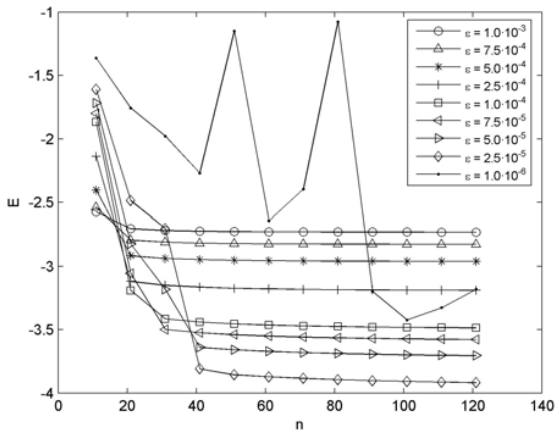

Fig. 15. Norm of error E, ε 10^{-3} to 10^{-6}, analysis case C2

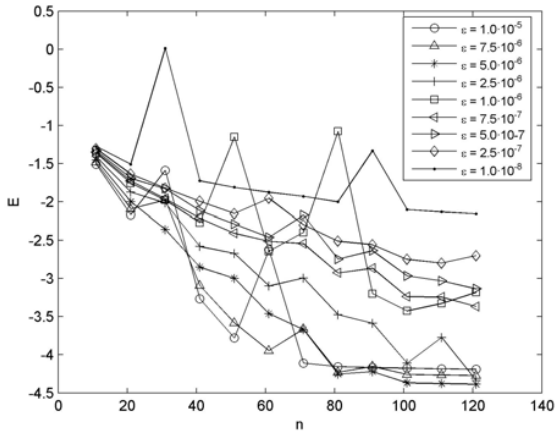

Fig. 16. Norm of error E, ε 10^{-5} to 10^{-8}, analysis case C2

The analysis with forcing term $g(x)$ confirms the expected behaviour after discussion of case B. For the two functions tested, when the perturbing parameter $\varepsilon << 1$ is moderately large, a fast convergence takes place for low orders of Bernstein basis, reaching a minimum of norm E. However, further increase of n has not significant impact on accuracy, see Fig. 11 and 15. In these cases, the assymptotic limit of norm E is lower the smaller the value of ε is. Convergent behavior is recovered if parameter ε is decreased, as illustrated in Fig. 12 and 16, where it can be observed that the numerical approximation needs larger orders n to reach its minimum computational error.

V. Conclusion

Inserted into a Galerkin implementation, Bernstein expansion can be used as an approximation technique yielding globally-supported shape functions that present interesting properties related to the consistency and the reproduction capability of the numerical approximation: analytical formulation, PU up to order 1 with regular distribution of evaluation points and able to span exactly the polynomial space, allowing the reproduction of any bounded continuous function by uniform convergence.

The presented work focuses on the study of the numerical performance of this global approximation for boundary value problems governed by perturbed constant-coefficient differential equations. Solutions to this type of problems typically exhibit boundary layer structure, which implies that the field variable suffers from abrupt gradients in thin regions in order to be able to adapt to the prescribed boundary conditions. Instead of local mesh refinement —or h-refinement— in boundary layer regions, which is a powerful strategy of mesh-based methods such as FEM for capturing high-order solutions, Bernstein-Galerkin approach employs patterns of equi-spaced evaluation points and is driven by p-refinement to reproduce the sharp gradients. Moreover, taking advantage of the analytical nature of Bernstein shape functions and their derivatives, a background integration mesh is not required for the evaluation of the terms of the system of discrete equations resulting from the Galerkin weak form of these problems.

Numerical experiments with benchmark problems of perturbation theory suggest that Bernstein-Galerkin approach can easily reach the accuracy of first and second-order uniform solutions of literature using a relatively low number of evaluation points. In some scenarios, when exact analytical solution is available, very accurate results may be achieved, but it those cases a phenomenon of lack of convergence may arise beyond the order of minimum error. As the perturbing parameter decreases, convergence is achieved by increasing the order of Bernstein basis, although rates of convergence become slower.

Acknowledgment

The author would like to thank the collaboration of Safran Group.

REFERENCES

[1] G.G. Lorentz, *Bernstein polynomials*, 2nd ed. Chelsea Publishing Company, 1986.
[2] G.R. Liu, *Mesh Free Methods. Moving beyond the Finite Element Method.* CRC Press, 2003.
[3] T.P. Fries, H.G. Matthies, *Classification and overview of meshfree methods.* (Informatikbericht-Nr. 2003-03). Brunswick: Technische Universität Braunschweig, 2004.
[4] E.H. Doha, A.H. Bhrawy, M.A. Saker, On the Derivatives of Bernstein Polynomials: An Application for the Solution of High Even-Order Differential Equations. *Hindawi Publishing Corporation Boundary Value Problems*, 2011.
[5] Ó.F Valencia, F.J. Gómez-Escalonilla, D. Garijo, J. López, Bernstein polynomials in EFGM. *Proc. IMechE Part C: J. Mechanical Engineering Science*, 2011, **225**(8), 1808-1815.
[6] M.I. Bhatti, P. Bracken, Solutions of differential equations in a Bernstein polynomial basis. *Journal of Computational and Applied Mathematics*, 2007, **205**, 272-280.
[7] N. Mirkov, B. Rasuo, A Bernstein Polynomial Collocation Method for the Solution of Elliptic Boundary Value Problems. *Cornell University Library*, 2012.
[8] J. Liu, Z. Zheng, Q. Xu, Bernstein-Polynomials-Based Highly Accurate Methods for One-Dimensional Interface Problems. *Journal of Applied Mathematics*, Volume 2012.
[9] P. Lancaster, K. Salkauskas, Surfaces generated by moving least squares methods *Math. Comput.*, 1981, **37**, 141-158.
[10] D. Garijo, Ó.F Valencia, F.J. Gómez-Escalonilla, J. López, Bernstein-Galerkin approach in elastostatics. *Proc. IMechE Part C: J. Mechanical Engineering Science*, Published online April 24, 2013, doi: 10.1177/0954406213486733.
[11] D. Gottlieb, S.A. Orszag, *Numerical Analysis of Spectral Methods: Theory and Applications.* Society for Industrial and Applied Mathematics. Philadelphia, Pennsylvania, 1977.
[12] C. Canuto, M.Y. Hussaini, A. Quarteroni, T.A. Zang, *Spectral Methods in Fluid Dynamics*, 2nd ed. Springer Series in Computational Physics. Springer-Verlag, 1988.
[13] T. Belytschko, Y.Y. Lu, L. Gu, Element-free Galerkin methods. *Internat. J. Numer. Methods Engrg.*, 1994, **37**, 229-256.
[14] J. Dolbow, T. Belytschko, An Introduction to Programming the Meshless Element Free Galerkin Method. *Arch. Comput. Meth. Eng.*, 1998, **5**(3), 207-241.
[15] T. Ohkami, E. Toyoshima, S. Koyama, Element Free Analysis on a Mapped Plane. *Proceedings of the Seventh International Conference on Computational Structures Technology*, In B.H.V. Topping, C.A. Mota Soares, (Editors), Civil-Comp Press, Stirlingshire, UK, Paper 126, 2004.
[16] Y. Suetake, Element-Free Method Based on Lagrange Polynomial. *J. Eng. Mech.*, 2002, **128**(2), 231-239.
[17] O.C. Zienkiewicz, R.L. Taylor, *The finite element method. The basis.*, 5th ed. Butterworth-Heinemann, 2000.
[18] K.E. Atkinson, *An introduction to numerical analysis*, 2nd ed. New York: John Wiley & Sons, Inc., 1988.
[19] C.M. Bender, S.A. Orszag, *Advanced Mathematical Methods for Scientists and Engineers*, McGraw-Hill Book Company, 1978
[20] M.Z. Spivey, Combinatorial Sums and Finite Differences. *Discrete Math.*, 2007, **307**, 3130-3146.
[21] K.W. Morton, D.F. Mayers, *Numerical Solution of Partial Differential Equations*, 2nd ed. Cambridge University Press, 2005.
[22] J.J.H. Miller, E. O'Riordan, G.I. Shishkin, *Fitted numerical methods for singular perturbation problems*, World Scientific, Singapore, 1996.
[23] C.J. Budd, G.P. Koomullil, A.M. Stuart, On the solution of convection-diffusion boundary value problems using equidistributed grids *SIAM J. Sci. Comput.*, 1998, **20**(2), 591-618.
[24] P. Knobloch, Numerical solution of convection-diffusion equations using upwinding techniques satisfying the discrete maximum principle. *Proceedings of the Czech-Japanese Seminar in Applied Mathematics 2005*, Kuju Training Center, Oita, Japan, September 15-18, 2005, 69-76.
[25] H.G. Roos, M. Stynes, L. Tobiska, *Robust Numerical Methods for Singularly Perturbed Differential Equations*, Springer, 2008.
[26] Y.N. Reddy, GBSL. Soujanya, K. Phaneendra, Numerical Integration Method for Singularly Perturbed Delay Differential Equations, *International Journal of Applied Science and Engineering*, 2012, **10**(3), 249-261.
[27] R.S. Johnson, *Singular Perturbation Theory, Mathematical and Analytical Techniques with Applications to Engineering*, Springer, 2005.
[28] E.J. Hinch, *Perturbation Methods*, Cambridge University Press, 1991.
[29] F. Verhulst, *Methods and Applications of Singular Perturbations*, Springer, 2005.

Diego Garijo is Aeronautical Engineer and PhD candidate by Universidad Politécnica de Madrid. He is currently working in Safran Group as Head of Training, R&D and Publications for Spain BU, CoC-Stress at Getafe. He has participated as stress analyst in numerous projects of the aerospace industry, including static, fatigue and damage tolerance certification of aircraft structures. His professional interests are mainly numerical simulation, computational mechanics, finite element analysis and meshless methods.